



1 **Effects of permafrost thaw on seasonal soil CO₂ efflux dynamics in a boreal
2 forest site**

3 Dragos A. Vas¹, Jaimie R. West², David Brodylo¹, Amanda J. Barker¹, William B. Baxter¹, and
4 Robyn A. Barbato²

5 ¹U.S. Army Engineer Research and Development Center-Cold Regions Research and Engineering
6 Laboratory, Ft. Wainwright, Alaska 99703, United States.

7 ²U.S. Army Engineer Research and Development Center-Cold Regions Research and Engineering
8 Laboratory, Hanover, New Hampshire 03755, United State.

9 *Correspondence to* Dragos Vas (Dragos.A.Vas@usace.army.mil) ORCID: 0009-0005-2319-5079.

10 **Abstract.** Permafrost regions in subarctic and arctic areas harbor substantial carbon reserves, which are
11 becoming increasingly vulnerable to microbial decomposition as soils warm. As the seasonally thawed
12 active layer deepens and anthropogenic disturbances escalate, accurately predicting carbon fluxes from
13 thawed permafrost requires a comprehensive understanding of soil respiration dynamics. This study
14 aimed to investigate the impact of disturbance on soil respiration rates and identify the key environmental
15 and geochemical factors influencing these processes in a boreal forest ecosystem near Fairbanks, Alaska.
16 The disturbed site demonstrated an increase in mean annual soil temperatures, recorded at $0.60 \pm 0.16^\circ\text{C}$,
17 along with a 14.4% rise in mean annual microbial activity, which peaked at 20% during the summer, in
18 contrast to the undisturbed site, which had a mean annual temperature of $-0.37 \pm 0.08^\circ\text{C}$. Furthermore,
19 bacterial and fungal community composition differed significantly between the two sites, suggesting a
20 potential mechanism underlying the variation in CO₂ efflux. Our research underscores the essential
21 importance of considering the rise in carbon emissions from anthropogenically disturbed soils in
22 permafrost areas, which are frequently neglected in assessments of the carbon cycle. This study
23 contributes to a deeper understanding of the complex interactions governing soil respiration in thawing
24 permafrost, ultimately informing more accurate predictions of carbon fluxes in these ecosystems.

25 **1. Introduction**

26 Soil respiration, the process by which carbon dioxide (CO₂) is released from the soil surface to
27 the atmosphere, is a critical component of the global carbon cycle. This process is influenced by the
28 microbial breakdown of organic material as well as the respiration of plant roots. Understanding soil
29 respiration dynamics is particularly crucial in boreal forests, as they encompass approximately 30% of the
30 global forest and play a vital role in global carbon sequestration (Bonan, 2008; Pan *et al.*, 2011; Chi *et al.*,
31 2021). Recent studies indicate that increasing temperatures could lead to boreal forests transitioning from
32 functioning as carbon sinks to becoming carbon sources (Bond-Lamberty *et al.*, 2018; Marty *et al.*, 2019,



33 Harel *et al.*, 2023). In boreal forests, soil respiration is estimated to contribute up to 68% of the total
34 ecosystem respiration (Parker *et al.*, 2020; Watts *et al.*, 2021) and is significantly impacted by changes in
35 soil temperature, soil moisture, the microbial community, and the type of vegetation present (Grace, 2004;
36 Fekete *et al.*, 2014; Rodtassana *et al.*, 2021). Soil respiration in permafrost regions is also influenced by
37 the deepening of the active layer (seasonal surface soil thaw) that may occur due to permafrost
38 degradation exacerbated by warmer soil and air temperatures (Turetsky *et al.*, 2020; Watts *et al.*, 2021).

39 Anthropogenic (e.g., trail development, firewood harvesting) and natural (e.g., wildfires,
40 flooding, drought) disturbances can significantly impact the terrain by altering the ground vegetation, as
41 well as soil temperature, structure, water content, organic matter content, and microbial communities,
42 thereby influencing the rates and patterns of soil respiration. Previous studies conducted in boreal forest
43 and spruce forest environments have shown that tree harvesting leads to a long-term increase in CO₂
44 effluxes due to a decrease in net radiation (Amiro 2001) and an increase in soil temperature (Gordon *et*
45 *al.*, 1987; Lytle and Cronan 1998; Amiro 2001) and soil water content because of vegetation cover loss
46 (Halim *et al.*, 2024). Tree harvesting also has a profound effect on the availability of substrates, both in
47 terms of quantity and quality, which subsequently modifies the biomass and structure of the microbial
48 community (Chatterjee *et al.*, 2008).

49 In a carbon dynamics study conducted in three boreal fen peatlands of Ontario, Canada, Webster
50 *et al.* (2023) discovered that drought conditions can significantly elevate CO₂ efflux while simultaneously
51 reducing the CH₄ efflux. Additionally, they found that shallow flooding can lead to a reduction in CO₂
52 emissions and an increase in CH₄ emissions. A separate investigation revealed that the flooding
53 significantly influenced the dynamics of CO₂ and CH₄ in riparian forests subject to varying degrees of
54 flooding. CO₂ emissions tend to rise with increased flood frequency, averaging 1.6 times higher in flood-
55 affected riparian forests compared to those protected from flooding, which exhibited unexpectedly strong
56 CH₄ sink characteristics (Jacinthe, 2015). Similar to the effects of flooding and drought, wildfires in
57 boreal forests significantly influence soil carbon efflux. Following the fire, the efflux of CO₂ from the soil
58 experienced a decline (Amiro, 2001; Koster *et al.*, 2017 and 2018; Halim *et al.*, 2024); however, it
59 subsequently rose over the course of several decades, ultimately peaking approximately 40 to 45 years
60 later. (Halim *et al.*, 2024).

61 Research on changes to soil respiration in disturbed environments is crucial to enhance our
62 understanding of the resilience and vulnerability of boreal forests to disturbances. As global temperatures
63 rise, the frequency and intensity of disturbances in these regions are expected to increase, potentially
64 leading to significant changes in soil carbon fluxes. Further, insights gained from such studies can inform



65 forest management practices aimed at mitigating the impacts of disturbances and preserving the carbon
66 sequestration potential of boreal forests.

67 The aim of this study is to measure and compare the soil respiration rates in an undisturbed
68 subarctic boreal forest with those in a subarctic boreal forest that has been affected by historical activities
69 tied to mining such as trail development and firewood harvest. These disturbances took place in the early
70 1900s, coinciding with the construction of a drainage ditch and an access trail to support mining
71 operations. Currently, there is no active drainage at the research site, and the trail is seldom used. The
72 study seeks to reveal the fundamental mechanisms of soil respiration in these ecosystems by examining
73 various edaphic factors, including soil temperature, moisture content, soil organic matter (SOM), pH, and
74 the composition of microbial communities. A Random Forest Model (RFM) was utilized in conjunction
75 with regression analysis to analyze the time series data, which encompassed variables such as soil
76 respiration, temperature, moisture, and air temperature. Furthermore, R statistical ANOVA analysis was
77 performed to evaluate soil characteristics, particularly pH and SOM, as well as the composition of soil
78 microbial communities. We hypothesize that there is a considerable escalation in carbon emissions from
79 anthropologically disturbed soils as compared to undisturbed soils in permafrost areas and we propose
80 that these emissions must be incorporated into models of carbon fluxes within these ecosystems.

81 **2. Materials and Methods**

82 **2.1 Site description**

83 The study was conducted at two adjacent sites underlain by permafrost in a subarctic boreal forest
84 located at the U.S. Army Cold Regions Research and Engineering Laboratory (CRREL) Permafrost
85 Research Tunnel Facility in Fox, Alaska (64.9507 N -147.6200 W, 248 m a.s.l.). The region experiences a
86 continental climate, which is defined by an average annual air temperature of -2.4°C , with average
87 temperatures in July reaching 16°C and January temperatures averaging -21.9°C ; extreme temperatures
88 throughout the year can range from -51°C to 38°C (Jorgenson et al. 2020). The two sites were situated
89 approximately 10 m apart; the first consists of an undisturbed black spruce forest ecosystem; the second
90 consists of an anthropogenically disturbed area where trails were established, and firewood was harvested
91 as part of mining activities in the region in the 1920's.

92 The vegetation at the undisturbed site consists of small black spruce (*Picea mariana*) ranging
93 from densely distributed to tightly spaced. Understory canopy is dominated by marsh and bog Labrador
94 tea (*Rhododendron tomentosum*; *groenlandicum*). Forest floor cover is primarily mosses (feather mosses
95 and *Sphagnum spp.*) and small shrubs including lowbush cranberry (*Vaccinium vitis-idaea*). The disturbed



96 site is characterized by scattered birch (*Betula neoalaskana*) and white spruce (*Picea glauca*) cover. The
97 understory canopy is primarily dwarf shrubs including marsh Labrador tea and bog blueberry (*Vaccinium*
98 *uliginosum*). The ground surface cover is dominated by grasses (*Poaceae*) and sedges (*Cyperaceae*). Soil
99 material types were classified as mineral soil (<20% OM; Soil Survey Staff, 2022) with more organic-rich
100 fractions (10-18% OM) comprising a surface layer (topsoil) and lower organic content (<5% OM) in the
101 stratigraphically deeper subsoil. The topsoil textures ranged from loam to silt loam, reflecting a higher
102 proportion of sand particles in the topsoil relative to the silt loam subsoil (SI Table 1).

103 **2.2 Data Collection**

104 Total soil respiration (autotrophic and heterotrophic), temperature, volumetric water content
105 (VWC), air temperature, and barometric pressure were measured from 4 Nov 2022 to 9 Nov 2023 at eight
106 plots; four plots were located at the undisturbed site and the remaining four at the adjacent disturbed site.
107 In preparation for total soil efflux measurements, a soil collar made from thick-walled polyvinyl chloride
108 (PVC) pipe was inserted at each of the eight plots. The collars had an inside diameter of 21.3 cm and a
109 height of 11.4 cm and were inserted 2-3 cm into the soil through the soil vegetation cover. Soil
110 temperature and VWC sensors were also installed in both the topsoil and subsoil layers at all plots.

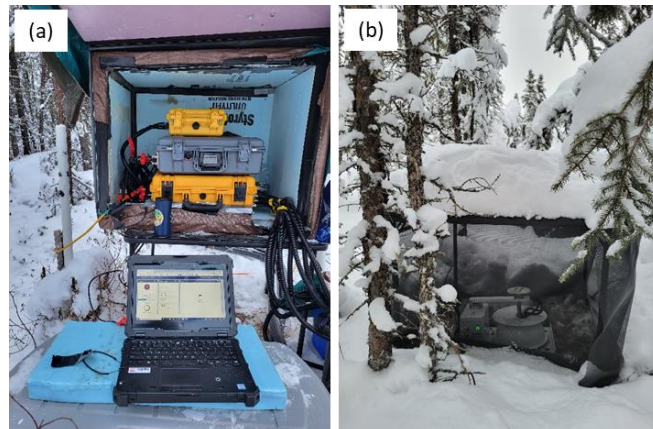
111 The varying temporal resolution soil parameter (30 min), weather (15 min), and soil efflux (30
112 min) data were averaged to hourly, daily, and seasonal means for statistical analyses. The seasons were
113 categorized as winter (November to March), spring (April to May), summer (June to August), and autumn
114 (September to October), based on the observed patterns of efflux seasonality at the research location. This
115 classification aligns with earlier studies on boreal forest efflux conducted by Wats et al. (2021) in Alaska
116 and Canada.

117 **2.3 Total soil CO₂ efflux measurements**

118 The total soil CO₂ efflux respiration, which encompasses the overall release of CO₂ from the soil
119 into the atmosphere (including both autotrophic and heterotrophic processes), was measured using a LI-
120 COR Soil gas flux system (LI-COR inc., Lincoln, Nebraska, USA) composed of 2 gas analyzers, LI-870
121 CO₂/H₂O analyzer and LI-7810 CH₄/CO₂/H₂O trace gas analyzer, a LI-8250 multiplexer, and eight 8200-
122 104 Opaque Long-Term Chambers. The two gas analyzers and multiplexer were housed in a custom-made
123 Styrofoam enclosure (Figure 1a) to protect them from precipitation and extreme winter temperatures. The
124 eight chambers were deployed over the soil covers installed at the study plots and were connected to the
125 multiplexer by a 15 m long tubing and cable assembly provided by the manufacturer. Minor adaptations
126 to the soil gas flux system were necessary to ensure data collection in the winter months; first the cable



127 and tubing assembly was wrapped in 1.3 cm thick tubular pipe insulation foam to prevent/minimize
128 clogging due to moisture freezing up inside the tubing, and second, Costco (Columbus, Indiana) folding
129 tables with a surface of 91.4 cm × 91.4 cm were positioned over the 8200-104 long-term chambers to
130 prevent snow accumulation on the chambers (Figure 1b). Therefore, all sample locations were equally
131 affected by the lack of snowfall and possible grazing by animals. A detailed description of the soil gas
132 flux system operation and winter modifications can be found in Vas *et al.* (2023).



133

134 **Figure 1. Custom modifications for LI-COR Soil gas flux system in cold climates. Specially designed**
135 **enclosures to ensure optimal operating temperatures (a) (photo credits: Dragos A. Vas, 17**
136 **November 2023), insulated tubing for instruments to prevent clogging, and long-term covers for**
137 **chambers (b) (photo credits: Dragos A. Vas, 17 November 2023) to inhibit snow accumulation or**
138 **drifting on the chambers.**

139

140 **2.4 Soil and meteorological condition measurements**

141 Soil temperature, VWC, air temperature, and barometric pressure were measured using the
142 following Onset HOBO (Onset, Bourne, Massachusetts, USA) instrumentation: U30 USB Weather
143 Station, S-TMB-M002 12-Bit Temperature Smart Sensor, S-SMC-M005 EC5 Soil Moisture Smart
144 Sensor, S-THC-M002 Temperature/Relative Humidity Smart Sensor, and S-BPB-CM50 Smart
145 Barometric Pressure Sensor. Soil temperature and VWC were recorded in the topsoil and subsoil layers,
146 approximately 30 cm from each long-term chamber, at a depth of 18.5 ± 1.19 cm in the topsoil layer and
147 34.5 ± 1.47 cm in the subsoil layer for the undisturbed site. At the disturbed site, the measurements were
148 taken at 13.5 ± 2.53 cm in the topsoil layer and 35.5 ± 1.85 cm in the subsoil layer. These depths were
149 measured from the top of the ground vegetation cover, which had a thickness of 16.5 ± 1.19 cm at the
150 undisturbed site and 9.5 ± 0.87 cm at the disturbed site. VWC measurements were restricted to the



151 summer and autumn seasons due to the sensor's inability to measure below freezing temperatures. Air
152 temperature and barometric pressure were measured at 2 m above the substrate surface.

153 The depth of thaw in the active layer was assessed at ~ 10 cm from each of the eight chamber
154 plots during each site visit (n = 160) from 12 May to 3 Oct 2023. To determine this depth, a graduated
155 metal rod with a diameter of 1 cm (known as a frost probe) was inserted into the ground, at the same
156 location, until it met resistance, establishing the distance between the ground surface vegetation and the
157 top of the frozen soils (Shiklomanov *et al.* 2013).

158 **2.5 Soil collection and property analysis**

159 Soil samples were collected from both the topsoil and subsoil layers across all plots in the autumn
160 (September 2022), winter (February 2023), and summer (June 2023) seasons to analyze potential
161 variations in microbial community composition among seasons, disturbance regimes, and soil layers. The
162 samples were collected at identical depths during each season, which coincided with the depth at which
163 the soil temperature and moisture probes were positioned; these depths varied for each plot. The winter
164 samples were acquired using a gas-powered SIPRE (Snow, Ice, and Permafrost Research Establishment)
165 corer (Jon's Machine Shop, Fairbanks, Alaska, USA). Nitrile gloves were utilized to minimize any
166 potential contamination to the cores. Furthermore, the SIPRE corer and all associated tools were
167 thoroughly sanitized with 70% isopropyl alcohol, DNA away, and RNase away (Thermo Fisher Scientific
168 in Waltham, MA, USA). The cores were then subsampled into approximately 5 cm long cylinders using a
169 sanitized hammer and chisel and were carefully placed into sterile Nasco™ Whirl-pak bags (Thermo
170 Fisher Scientific, Waltham, MA, USA); further information on this sampling method can be found in
171 Barbato *et al.* (2022). Summer and autumn soil samples were gathered using a sanitized trowel with 70%
172 isopropyl alcohol, DNA away, and RNase away. The samples, approximately 5 cm thick, were placed in
173 sterile Nasco™ Whirl-pak bags and immediately placed in a cooler with frozen ice packs, then transferred
174 to a freezer upon arrival at the Cold Regions Research and Engineering Laboratory in Fairbanks, Alaska
175 (CRREL-AK). All collected soil samples were kept at a temperature of -25 °C until shipped to CRREL in
176 Hanover, New Hampshire (CRREL-NH), where they were stored at -20 °C until further processing.

177 Loss on ignition (LOI) was measured as a proxy for soil organic matter (SOM) content (Storer,
178 1984) on all soil samples. Here, LOI is the proportion of mass loss from oven-dried soil (dried at 105 °C
179 for 24 hours) following 2 hours at 360 °C in a muffle furnace. Soil total carbon and total nitrogen was
180 measured via combustion using a TruSpec C and N Analyzer (LECO, St. Joseph, MI, USA) at the
181 University of Wisconsin Soil and Forage Lab. Soil pH was measured from a 1:1 slurry of soil:CaCl₂
182 solution (0.01M) using a pH probe (Hanna Instruments, Woonsocket, RI, USA) and a SevenEasy S20 pH



183 meter (Mettler Toledo, Columbus, OH, USA). Soil pH was converted to H⁺ concentration prior to taking
184 an average or statistical analysis. LOI total carbon, total nitrogen and soil pH was statistically analyzed
185 using ANOVA in R.

186 **2.6 Soil microbial DNA extraction, gene sequencing, and data analysis**

187 Soil was partially defrosted and homogenized in the sample bag prior to subsampling 250 mg into
188 bead beating tubes. Total genomic DNA was extracted using the DNeasy PowerSoil Pro Kit (Catalog No.
189 47014, Qiagen, Germantown, MD, USA), using a Precellys Evolution Touch homogenizer for the bead
190 beating step (Catalog number P002511-PEVT0-A.0, Bertin Technologies, Montigny-le-Bretonneux,
191 France). Automated DNA extraction was done with a QIAcube Connect (Catalog No. 9002864, Qiagen,
192 Germantown, MD, USA) and each extraction run included a blank. Extracted DNA was held at -20 °C.

193 Library preparation and sequencing was completed at Argonne National Laboratory (Lemont, IL,
194 USA), as follows. For bacterial analysis, the V4 region of the 16S rRNA gene was targeted for PCR
195 amplification with region-specific primers (forward primer 515F and reverse primer 806R); and for
196 fungal analysis, the ITS region was amplified using appropriate barcoded primers (Caporaso *et al.*, 2011;
197 Caporaso *et al.*, 2012; Apprill *et al.*, 2015; Parada *et al.*, 2016; Smith *et al.*, 2014; Walters *et al.*, 2016).
198 Each PCR reaction contained 1 µL template DNA, 12.5 µL AccuStart II PCR ToughMix (Quantabio,
199 Beverly, MA, USA), 1 µL forward primer with Golay barcode (5 µM concentration), 1 µL reverse primer
200 (5 µM concentration), and 9.5 µL DNA-free PCR water. PCR conditions were: 94 °C (3 minutes to
201 denature the DNA); 35 cycles of 94 °C (45 s), 50 °C (60 s), and 72 °C (90 s); final extension at 72 °C (10
202 minutes). PCR product was quantified using Quant-iT PicoGreen (P7589, Invitrogen, Waltham, MA,
203 USA). Equimolar amounts of amplicons were pooled, purified using AMPure XP Beads (A63881,
204 Beckman Coulter, Brea, CA, USA), quantified (Qubit, Invitrogen), and diluted to 6.75 pM using a 10%
205 PhiX spike. Paired-end 2 x 251 sequencing was done on a MiSeq (Illumina, San Diego, CA, USA).

206 Sequencing data were processed in R (R-Core-Team, 2018), using a dada2 v1.18.0 pipeline
207 (Callahan *et al.*, 2016), as in Baker *et al.* (2023), implemented using Snakemake v7.25.0 (Mölder *et al.*,
208 2021). Taxonomy assignment was based on the SILVA 138.1 reference database for 16S sequences (Quast
209 *et al.*, 2013; Yilmaz *et al.*, 2013) and the UNITE database (release 25.07.2023) for ITS sequences (Kölgalg
210 *et al.*, 2013; Nilsson *et al.*, 2019). Chloroplasts and mitochondria were excluded from the dataset. A total
211 of 2836 fungal ASVs and 10,608 bacterial ASVs were identified (excluding extraction blanks). Amplicon
212 sequences are in the National Center for Biotechnology Information Sequence Read Archive (NCBI
213 SRA), accession PRJNA1178745. Though our bacterial primers targeted both bacterial and archaeal 16S
214 rRNA, we will refer simply to bacteria, which comprise 99.8% of total reads. Of archeal reads, 80%



215 represented the phylum *Crenarchaeota*. One sample was excluded from analysis because it was
216 mislabeled (2023_Feb, Chamber 3, Organic).

217 R (R-Core-Team, 2018), and *ggplot2* (Wickham, 2016) were used for data analysis and
218 visualization; the bioinformatic approach followed West *et al.* (2022). Community composition was
219 visualized using principal coordinates analysis (PCoA) of Bray-Curtis dissimilarities (Bray and Curtis,
220 1957) generated using *avgdist* from the R package *vegan* (Oksanen *et al.*, 2024) using rarefaction (999
221 iterations) to a sampling depth of 16,300 for 16S and 6150 for ITS. A significant effect ($p < 0.05$) of
222 disturbance, sampling date, and interaction of these factors on community composition was tested within
223 each soil layer (topsoil and subsoil), using permutational multivariate analysis of variance
224 (PERMANOVA; *adonis2* from *vegan*) (Anderson, 2001). Richness was evaluated using weighted linear
225 regression (*betta* function in *breakaway* R package) (Willis *et al.*, 2017), and a significant effect of
226 disturbance tested via ANOVA. Differential abundance (*differentialTest* in the *corncob* package) (Martin
227 *et al.*, 2021) was then used to identify significant enrichment or depletion of individual taxa due to
228 disturbance, after excluding taxa with mean relative abundance < 0.00001 .

229 **2.7 Random Forest modeling**

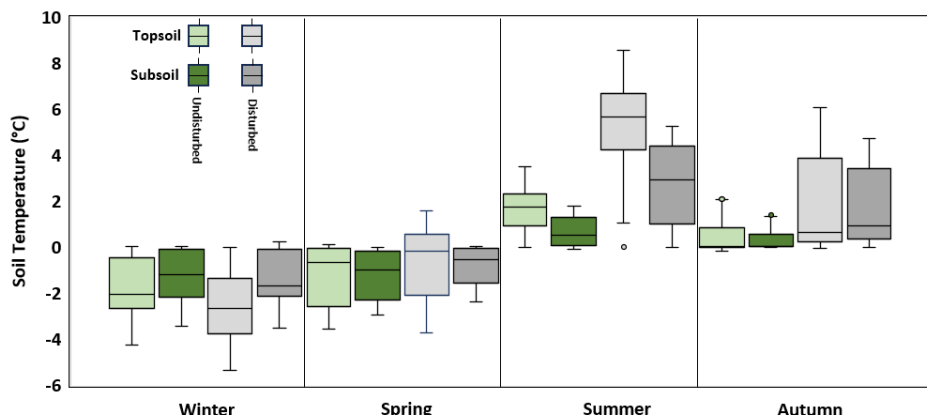
230 A regression-based Random Forest (RF) model developed in R was used to identify the relative
231 importance of the input variables to predict hourly and daily CO₂ concentrations. RF was chosen over
232 other algorithms due to its wide and successful application in determining variable importance
233 (Behnamian *et al.*, 2017; Lei *et al.*, 2024). In RF, the supervised non-linear algorithm can combine
234 predictions from hundreds or thousands of individual decision trees via bootstrap aggregation to generate
235 an ideal output (Schonlau and Zou, 2020). Compared with individual decision trees, this results in an
236 increase in generalization accuracy and a reduction in overfitting. A repeated k-fold cross-validation
237 technique was also employed. In this technique, data are randomly separated into k subsets with $k-1$ used
238 to train the model and the remainder to test the model, which is then repeated a specified amount. We
239 selected a value of 10 for k and a value of 5 for repetition. Input variables were the same for each instance
240 except barometric pressure being dropped for daily CO₂ concentrations due to poor importance values.
241 Thaw depth was static in the dataset that the model used from 4 October through 16 May due to the
242 presence of a frozen surface layer preventing thaw depth probing. Organic soil VWC and mineral soil
243 VWC from 1 November – 31 March and 1 April – 31 May were omitted for machine learning due to the
244 inability of the probes to function properly in subzero temperatures.

245 **3. Results**



246 **3.1 Soil conditions**

247 Soil temperature fluctuated by a factor of three at the disturbed site and by a factor of 1.9 at the
248 undisturbed site over the course of the year. The undisturbed and disturbed sites exhibited contrasting
249 thermal regimes. At the undisturbed site, the mean annual soil temperatures were below freezing,
250 exhibiting -0.33 ± 0.1 °C for topsoil and -0.41 ± 0.07 °C for subsoil (Figure 1). In contrast, the disturbed
251 site experienced positive mean annual soil temperatures, with 0.72 ± 0.2 °C for topsoil and 0.48 ± 0.13 °C
252 for subsoil. Winter was the only season with warmer topsoil and subsoil temperatures at the undisturbed
253 site. For both the undisturbed and disturbed sites, the subsoil layer was cooler than the topsoil layer in
254 terms of mean annual temperature. Significantly warmer soil temperatures were observed at the disturbed
255 site during the summer (4.04 ± 0.19 °C; $p < 0.001$, ANOVA) and autumn (1.88 ± 0.23 °C; $p < 0.001$,
256 ANOVA) in comparison to the temperatures recorded at the undisturbed site during the same seasons.
257 Conversely, the mean summer temperature at the undisturbed site was 1.15 ± 0.08 °C, while the mean
258 autumn temperature was 0.38 ± 0.07 °C (Figure 2). Soil temperatures in the shallower topsoil layer
259 exhibited greater variability throughout the year compared to the temperatures in the deeper subsoil layer
260 at both sites (Figure 2).



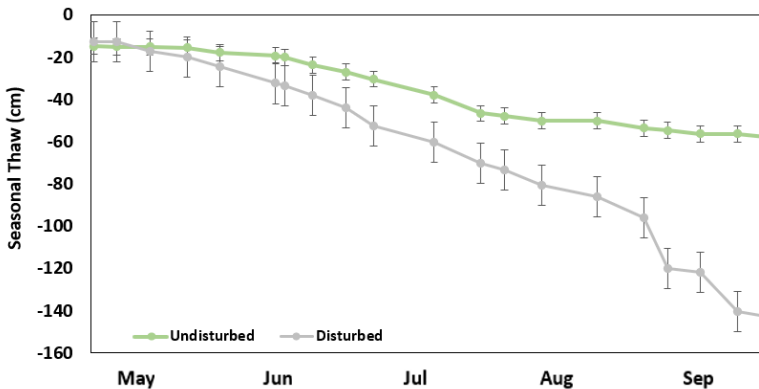
261
262 **Figure 2. Seasonal soil temperature patterns.** The seasons were delineated as winter (Nov–Mar),
263 spring (Apr and May), summer (Jun–Aug), and autumn (Sep and Oct). Soil temperature are
264 average daily values from the topsoil and subsoil layers at the 8 chamber plots: 4 at the undisturbed
265 site and 4 at the disturbed site. The range of the boxplot represents the first and third quartiles,
266 while the central line signifies the median. The whiskers of the box extend to the minimum and
267 maximum values, with outliers represented by circles.

268

269 VWC values ranged from 0.29 ± 0.00 m³/m³ to 0.47 ± 0.00 m³/m³ (1 Jun to 31 Oct 2024) (SI
270 Figure S1). Subsoil layer exhibited elevated mean seasonal VWC values, as compared to the topsoil



271 layer, at both locations (p values from 0.04 to < 0.001 , ANOVA). Average maximum seasonal thaw depth
272 exhibited significant differences between the two locations (p values 0.02, ANOVA), ranging from 58 ± 3
273 cm or 143 ± 29 cm at the undisturbed site or disturbed site, respectively (Figure 3). While the maximum
274 seasonal thaw depth remained relatively consistent across the undisturbed plots, ranging from 50 cm to 61
275 cm, the disturbed plot displayed a larger range in maximum thaw depth, varying from 82 cm to 204 cm.



276

277 **Figure 3. Average seasonal thaw depth at the undisturbed and disturbed sites measured using**
278 **manual frost probe measurements from 12 May to 3 Oct 2023. Error bars are standard error.**

279

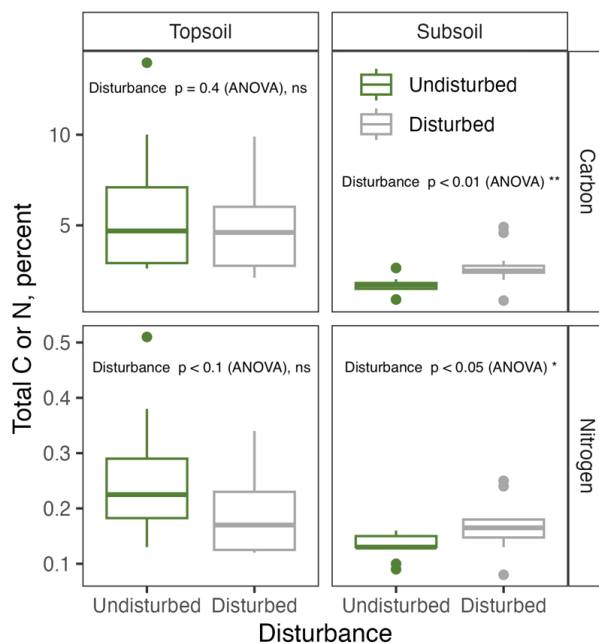
280 3.2 Soil properties

281 The disturbance treatment had a significant effect on LOI (a proxy for SOM content) in the
282 subsoil layer, but not the topsoil layer (SI Figure S2). There was no significant effect of sampling date or
283 significant interaction of sampling date and disturbance on LOI. Mean total C content for subsoil in the
284 disturbed treatment was 2.7% (averaged across LiCor chamber plots and sampling dates), significantly
285 greater than that of the undisturbed treatment mean of 1.7% ($p < 0.01$; ANOVA). Mean LOI for the
286 topsoil layer was 0.122 and 0.142 for disturbed and undisturbed, respectively (not significant).

287 Similarly, the disturbance treatment was a significant factor for soil total C content and total N
288 content in the subsoil layer ($p < 0.01$ and $p < 0.05$, respectively; ANOVA), but not the topsoil layer
289 (Figure 4), and there was no significant effect of sampling date or significant interaction of sampling date
290 and disturbance on either C or N. Mean total C content for subsoil in the disturbed treatment was 2.7%
291 (averaged across LiCor chamber plots and sampling dates), significantly greater than that of the
292 undisturbed treatment mean of 1.7% ($p < 0.01$; ANOVA). Mean total C content for the topsoil layer was
293 4.7% and 5.8% for disturbed and undisturbed, respectively (not significant). Mean total N content for



294 subsoil in the disturbed treatment was 0.16%, significantly greater than that of the undisturbed treatment
295 mean of 0.13% ($p < 0.01$; ANOVA). Mean total N content for the topsoil was 0.19% and 0.25% for
296 disturbed and undisturbed, respectively (not significant).



297

298 **Figure 4. Soil total carbon and total nitrogen, by disturbance treatment. Boxplots represent all**
299 **three sampling dates and four LiCor chamber plots, within each disturbance treatment.**

300

301 Similar to the response of LOI, total C, and total N, soil pH was significantly different in the
302 subsoil layer, depending on disturbance treatment; the effect of disturbance on the topsoil layer was not
303 significant (SI Figure S3). There was no significant effect of sampling date or significant interaction of
304 sampling date and disturbance on soil pH. Mean pH for subsoil in the disturbed treatment was 4.63
305 (averaged across chambers and sampling dates), significantly greater than that of the undisturbed
306 treatment mean of 4.11 ($p < 0.01$; ANOVA). Mean pH for the topsoil layer was 3.78 and 3.79 for
307 disturbed and undisturbed, respectively (not significant).

308 **3.3 Soil microbial community composition and diversity**

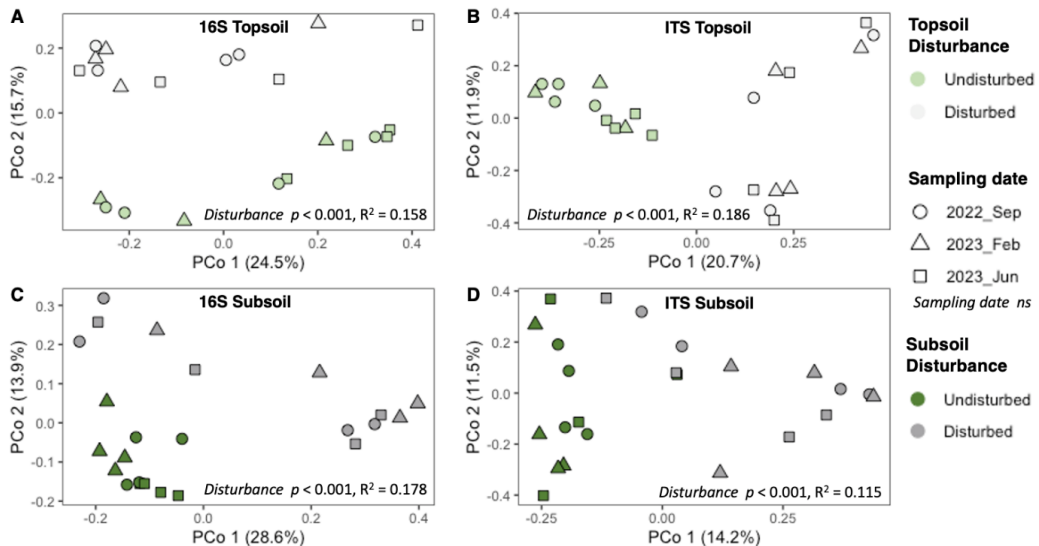
309 We analyzed the effect of disturbance on microbial community composition and diversity to
310 better understand the microbial role in soil respiration. The dominant bacterial phyla included



311 *Proteobacteria*, *Acidobacteria*, *Actinobacteria*, *Verrucomicrobia*, and *Chloroflexi*, which together
312 comprised over 75% of relative abundance (SI Figure S4). For fungi, 54% of relative abundance was
313 comprised of *Ascomycota* (mostly classes *Leotiomycetes* and *Archaeorhizomycetes*), and 40% was
314 *Basidiomycota* (mostly class *Agaricomycetes*) (SI Figure S5). Differential abundance testing only
315 identified several dozen taxa (after filtering for somewhat higher abundance taxa) that were either
316 significantly enriched or depleted under disturbance (see SI Figures S6 and S7). Notably, several
317 *Chloroflexi* and *Dormibacterota* (a newly named phylum, previously identified as *Chloroflexi*) ASV's are
318 depleted under disturbance relative to the undisturbed condition in subsoil, particularly at the February
319 sampling date (SI Figure S6).

320 Mean estimated bacterial richness across the dataset was 711.5 ASVs, with a significant effect of
321 disturbance (SI Figure S8). Overall, the disturbed samples had 30% higher richness compared to the
322 undisturbed samples ($p < 0.01$, ANOVA); within each date and soil layer combination, only the February
323 2023 subsoil samples demonstrated a significant effect of disturbance ($p < 0.01$, ANOVA). There was no
324 effect of sampling date or soil layer, or interaction amongst the factors. Mean estimated fungal richness
325 across the dataset was 165 ASVs; there was no effect of disturbance, sampling date, soil layer, or
326 interaction amongst the factors (SI Figure S8).

327 Using Bray-Curtis dissimilarities to evaluate beta diversity (Figure 5), there was a significant
328 effect of disturbance regime on both bacterial and fungal communities in both topsoil and subsoil layers
329 ($p < 0.001$ for all; $R^2 = 0.158, 0.178, 0.186, 0.115$ for bacterial topsoil, bacterial subsoil, fungal topsoil,
330 and fungal subsoil communities, respectively; PERMANOVA). Sampling date did not have a significant
331 effect.



332

333 **Figure 5. Principal coordinates analysis of Bray-Curtis dissimilarity data**
334 following rarefaction. Panels (A) and (C) represent the bacterial community (16S marker), and
335 panels (B) and (D) represent the fungal community composition (ITS marker). The top panels (A &
336 B; lighter shades) represent the topsoil layer community composition, while the bottom panels (C &
337 D; darker shades) represent the subsoil community composition.

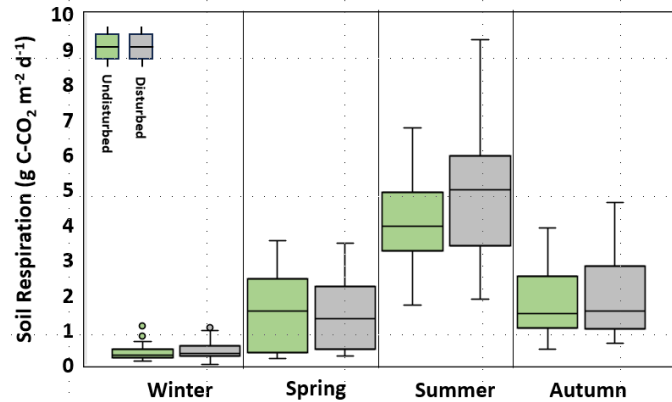
338

339 **3.4 Soil Respiration**

340 The total soil respiration showed strong seasonal and disturbance level patterns. The undisturbed
341 site had an average annual soil efflux of 1.81 ± 0.09 g C-CO₂ m⁻² d⁻¹, while the disturbed site had an
342 average annual soil efflux of 2.07 ± 0.11 g C-CO₂ m⁻² d⁻¹. On July 20, the undisturbed site recorded the
343 highest average daily flux of 9.27 g C-CO₂ m⁻² d⁻¹. The peak seasonal soil efflux occurred during the
344 summer season (SI Figure S9), with seasonal mean daily fluxes reaching 4.01 ± 0.12 g C-CO₂ m⁻² d⁻¹ at
345 the undisturbed and 4.81 ± 0.17 g C-CO₂ m⁻² d⁻¹ at the disturbed site ($p < 0.0001$, ANOVA; Figure 6).
346 This was followed by autumn, where seasonal mean values were lower at 1.79 ± 0.13 g C-CO₂ m⁻² d⁻¹ at
347 the undisturbed and 1.91 ± 0.15 g C-CO₂ m⁻² d⁻¹ at the disturbed (not statistically different). Spring
348 showed a decrease with 1.46 ± 0.14 g C-CO₂ m⁻² d⁻¹ at the undisturbed and 1.41 ± 0.13 g C-CO₂ m⁻² d⁻¹ at
349 the disturbed site (not statistically different), while the lowest efflux was recorded during winter with 0.33
350 ± 0.01 g C-CO₂ m⁻² d⁻¹ at the undisturbed and 0.39 ± 0.13 g C-CO₂ m⁻² d⁻¹ at the disturbed site ($p < 0.01$,
351 ANOVA). CO₂ flux was significantly different between the undisturbed and disturbed sites in the winter
352 ($p = 0.01$ ANOVA) and summer ($p < 0.01$, ANOVA) and revealed no statistically significant efflux
353 differences between the two sites in the shoulder seasons.



354



355

Figure 6. Seasonal soil respiration patterns observed at the undisturbed and disturbed sites. Soil respiration emissions are average daily fluxes from the 8 long-term chambers: 4 at undisturbed site and 4 at disturbed site. The range of the boxplot represents the first and third quartiles, while the central line signifies the median. The whiskers of the box extend to the minimum and maximum values, with outliers represented by circles.

360

361 3.5 Linear regression analysis to determine important variables contributing to soil efflux

362

A linear regression analysis was performed on the mean daily averages to investigate the seasonal correlation between soil efflux and various factors, including air temperature, barometric pressure, seasonal thaw depth, topsoil and subsoil temperature, and volumetric water content (VWC) at both undisturbed and disturbed sites. The presence of disturbance did not have a significant effect (p values 0.3 to 0.9, ANOVA) on the relationship between soil efflux and the aforementioned variables between the two sites. The analysis revealed that overall soil and air temperature exhibited the strongest correlation with soil respiration across all sites during different seasons. Soil and air temperatures showed the strongest correlations with soil efflux across all seasons. Seasonal R^2 values for soil temperatures ranged from 0.21–0.65 (winter), 0.87–0.92 (spring), 0.52–0.79 (summer), and 0.85–0.93 (autumn). Air temperature also correlated strongly with soil efflux in spring ($R^2 = 0.74$ –0.77) and autumn ($R^2 = 0.83$ –0.87). Moderate correlations were observed between soil efflux and thaw depth at both sites, with R^2 values ranging from 0.39–0.50 in spring, 0.41–0.43 in summer, and 0.74 in autumn.

374

The correlation between soil efflux and topsoil and subsoil VWC varied during the summer and fall seasons, as well as across the two soil layers. At the undisturbed site, in summer, moderate correlation was found in the topsoil ($R^2 = 0.38$) and strong in the subsoil ($R^2 = 0.69$). In autumn, correlations were strong in the topsoil ($R^2 = 0.62$) but weaker in the subsoil ($R^2 = 0.22$). At the disturbed site, in summer, the correlation was weak in the topsoil ($R^2 = 0.09$) but strong in the subsoil ($R^2 = 0.64$). In autumn, weak



379 correlations were observed in both layers ($R^2 = 0.28$ in topsoil and 0.10 in subsoil). Regression analysis
380 showed weak to no correlation between soil efflux and barometric pressure during winter and autumn (R^2
381 = 0.02–0.12) and no correlation in spring and summer. A slightly higher correlation was noted in winter
382 when using hourly averages ($R^2 = 0.23$ undisturbed, 0.18 disturbed).

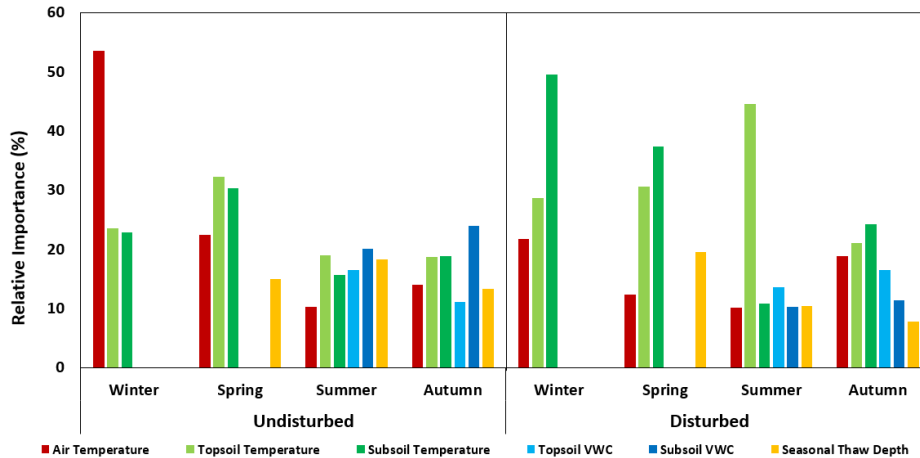
383 **3.6 Random forest efflux modeling**

384 The RF model accurately described the effects of disturbance with the variation in soil respiration
385 at both locations, showing strong confidence levels with high R^2 and moderate to low mean absolute error
386 (MAE) values. Specifically, the model's R^2 values and corresponding MAE were 0.95 (0.14 MAE) for
387 winter, 0.80 (0.38 MAE) for spring, 0.94 (0.16 MAE) for summer, and 0.82 (0.04 MAE) for autumn at the
388 undisturbed site, and 0.95 (0.12 MAE) for winter, 0.83 (0.52 MAE) for spring, 0.96 (0.13 MAE) for
389 summer, and 0.84 (0.05 MAE) for autumn at the disturbed site.

390 The predictors' relative importance (RI) varied across seasons and sites (Figure 7). In the winter
391 model at the undisturbed site, air temperature emerged as the most influential predictor, accounting for
392 53.6% RI. Conversely, at the disturbed site, the subsoil temperature exhibited the highest predictive power
393 with 49.6% RI (figure 7). For the spring model, soil temperature was the best predictor at both sites, the
394 topsoil layer temperature exhibited a slightly greater predictive power at the undisturbed site, whereas the
395 subsoil layer temperature proved to be more influential at the disturbed site. In the undisturbed site's
396 summer model, the soil moisture and temperature as well as the seasonal thaw depth variables exhibit
397 similar RI values, ranging from 15.7 to 20.2%. Among these variables, air temperature has the lowest
398 predictive power, with an RI of 10.3%. Conversely, at the disturbed site, the topsoil layer temperature
399 stands out as the strongest predictor, with an RI of 44.6%. It is followed by the topsoil VWC, which has
400 an RI of 13.7%. The undisturbed site's autumn model indicates that subsoil layer VWC has the highest
401 predictive power at 24.3% RI, followed by subsoil layer temperature at 18.9% RI, and topsoil layer
402 temperature at 18.7% RI. However, the disturbed autumn model shows that subsoil layer temperature is
403 the most influential factor in predicting CO₂ efflux with 24.3% RI and topsoil layer (21.1% RI) and air
404 (18.9% RI) also playing significant roles.



405



406

407 **Figure 7. Relative importance (%) of variables to predict CO₂ efflux. Missing or static input**
variables were not measured for importance.

408

409 Throughout the different seasons, various factors contribute to the varying degrees of relative
410 importance regarding soil respiration. These factors include air temperature, the temperature of both
411 topsoil and subsoil layers, and volumetric water content, which pertains only to subsoil. This information
412 is presented in Table 1.

413

414 **Table 1. Tabulation of the most important predictor variables to explain variability in the soil efflux**
415 data between disturbed and undisturbed sites as a function of season.

Season	Plot	Highest Predictor	RI
Winter	Undisturbed	Air temperature	53.6
Winter	Disturbed	Soil layer temperature (subsoil)	49.6
Spring	Undisturbed	Soil layer temperature (topsoil)	32.2
Spring	Disturbed	Soil layer temperature (subsoil)	37.4
Summer	Undisturbed	Volumetric water content (topsoil)	20.2
Summer	Disturbed	Soil layer temperature (topsoil)	44.6
Autumn	Undisturbed	Volumetric water content (subsoil)	24.0
Autumn	Disturbed	Soil layer temperature (subsoil)	24.3

416

417 4. Discussion



418 Our findings show that the temperatures of the active layer soil are markedly elevated at the
419 disturbed site in comparison to the undisturbed site. Previous research has indicated that this increase in
420 temperature is primarily due to a decrease in insulating organic matter (Gordon *et al.*, 1987; Lytle and
421 Cronan, 1998; Amiro, 2001; Halim *et al.*, 2024) and alterations in surface albedo resulting from
422 disturbance (Amiro, 2001). The consequences of these modified thermal conditions are significant, as
423 heightened soil temperatures may expedite permafrost degradation and affect biogeochemical cycles
424 (Chatterjee *et al.*, 2008) contributing to a positive feedback cycle. It stands to reason that winter was the
425 only season during which soil temperatures were elevated regardless of organic content at the undisturbed
426 site (Figure 2), as the unaltered surface vegetation provided a layer of insulation against the low air
427 temperature. Furthermore, disturbance notably influenced total C, total N (Figure 4), and soil pH within
428 the subsoil layer.

429 The effects of disturbance on microbial communities were substantial, with significant alterations
430 noted in both bacterial and fungal compositions. Notably, the date of sampling did not exert a significant
431 impact on community structure, indicating that the disturbance itself serves as the principal factor driving
432 these changes. This finding is consistent with earlier studies that suggest soil disturbances can disrupt
433 microbial habitats, resulting in a reorganization of community dynamics (Chatterjee *et al.*, 2008). Such
434 changes can lead to cascading effects on ecosystem functions, including nutrient cycling and the
435 decomposition of organic matter. We found that the disturbance-driven changes, led to higher average soil
436 temperatures and increased concentrations of mean SOM (LOI) (by a factor of 1.8) (SI Figure S2), mean
437 total carbon (by a factor of 1.6) (Figure 4), and mean total nitrogen (by a factor of 1.2) (Figure 4) in the
438 subsoil which positively influenced the mean annual soil respiration rates, resulting in a 14.4% increase
439 when compared to the undisturbed site.

440 The variability in soil efflux data between disturbed and undisturbed sites as a function of season
441 reveals distinct patterns influenced by key abiotic factors. In winter, air temperature emerged as the most
442 significant predictor for the undisturbed sites, likely due to its direct impact on microbial activity and
443 respiration rates. In contrast, the disturbed site during the same season showed a stronger correlation with
444 the subsoil layer temperature, suggesting that disturbances may alter the thermal dynamics of the soil
445 profile, making soil temperature a more crucial determinant. During spring, topsoil layer temperature was
446 the primary predictor for the undisturbed site, highlighting the importance of organic matter
447 decomposition driven by temperature changes. For the disturbed site, the subsoil layer temperature
448 remained the dominant factor, indicating that disturbances may have disrupted the organic layer, shifting
449 the focus to the subsoil layer's thermal conditions.



450 In the summer months, the volumetric water content in the subsoil layer emerged as the principal
451 predictor for the undisturbed site, highlighting the essential role of moisture availability in influencing
452 microbial activity and respiration during this warmer period. Conversely, the disturbed site exhibited a
453 more pronounced correlation with the temperature of the topsoil layer, indicating that disturbances may
454 have modified the soil's hydrological characteristics by increasing thaw depth and enhancing drainage,
455 which resulted in a reduced volumetric water content and rendered temperature a more significant factor
456 than moisture. As autumn approached, the volumetric water content in the subsoil layer reestablished
457 itself as the key predictor for the undisturbed site, reaffirming the ongoing significance of moisture for
458 microbial functions as temperatures began to decline. In contrast, for the disturbed site, the temperature of
459 the subsoil layer continued to be the prevailing influence, underscoring the enduring effects of
460 disturbances on the thermal dynamics of the soil.

461 Overall, the observed patterns indicate that soil disturbances fundamentally alter the relationships
462 between abiotic factors and CO₂ efflux. By reshaping thermal profiles and hydrological properties,
463 disturbances intensify microbial activity across seasons, thereby increasing CO₂ emissions.

464 Conclusion

465 As warming continues, thawing permafrost and degrading pristine areas in arctic and sub-arctic
466 regimes, there will be a higher degree of ecological response that occurs, particularly related to soil
467 respiration. Areas that, in theory, are undisturbed will begin to mirror anthropogenically disturbed areas in
468 terms of greenhouse gas efflux. This study provided valuable insights into the effects of disturbance on
469 critical soil properties and their influence on soil respiration. Our research indicates notable changes in
470 soil temperature, volumetric water content, the composition of bacterial and fungal communities, total
471 mean SOM, C and N levels and pH values in the subsoil layer, and the depth of the active layer as a result
472 of disturbances, which subsequently led to higher soil respiration rates. Soil respiration was primarily
473 regulated by temperature, (air and soil) while factors such as soil volumetric water content and the depth
474 of the active layer also contributed, with their relative importance varying throughout the different
475 seasons. These findings underscore the complex interplay between seasonal variations, soil disturbance,
476 and abiotic factors in determining soil respiration rates. Understanding these relationships is essential for
477 accurate modeling of carbon cycling and for developing effective strategies to mitigate the impacts of soil
478 disturbances on ecosystem functions. Both natural and anthropogenic disturbances can lead to a marked
479 rise in the emission of carbon dioxide and other greenhouse gases into the atmosphere. Neglecting to
480 account for these disturbances may result in a considerable underestimation of the role of soils in global



481 carbon cycles. Future investigations should concentrate on the long-term consequences of these dynamics,
482 especially considering ongoing warming change and its impact on permafrost regions.

483 *Data availability.* The datasets produced and/or examined in the present study can be obtained from the
484 corresponding author upon reasonable request.

485 *Author Contributions.* DAV conceptualized the study and managed the data collection, RAB provided
486 funding, DAV, AJB, and WBB collected the soil samples, DAV and DB performed the soil respiration
487 analysis, JRW performed the soil property and microbial community analyses. DAV drafted the initial
488 manuscript and all authors contributed to revisions.

489 *Competing Interests.* The authors have no relevant financial or non-financial interests to disclose.

490 *Acknowledgements.* The authors express their gratitude to Ms. Elizabeth Corriveau for her work in
491 conducting quality assurance and quality control on the soil respiration time series data and to Ms. Anne
492 Katula for her efforts in processing the soil samples for analyses related to microbial composition and soil
493 properties.

494 *Financial support.* This work was founded by PE 0602144A Program Increase ‘Defense Resiliency
495 Platform Against Extreme Cold Weather’.

496 **References**

497 Amiro, B.D., 2001. Paired-tower measurements of carbon and energy fluxes following disturbance in the
498 boreal forest. *Global Change Biology*, 7(3), pp.253-268.

499 Anderson, M.J., 2001. A new method for non-parametric multivariate analysis of variance. *Austral
500 ecology*, 26(1), pp.32-46.

501 Apprill, A., McNally, S., Parsons, R. and Weber, L., 2015. Minor revision to V4 region SSU rRNA 806R
502 gene primer greatly increases detection of SAR11 bacterioplankton. *Aquatic Microbial Ecology*,
503 75(2), pp.129-137.

504 Baker, C.C.M., Barker, A.J., Douglas, T.A., Doherty, S.J. and Barbato, R.A. 2023 Seasonal variation in
505 near-surface seasonally thawed active layer and permafrost soil microbial communities *Environ
506 Res Lett* **18** 055001



507 Barbato, R.A., Jones, R.M., Douglas, T.A., Doherty, S.J., Messan, K., Foley, K.L., Perkins, E.J., Thurston,
508 A.K. and Garcia-Reyero, N., 2022. Not all permafrost microbiomes are created equal: Influence
509 of permafrost thaw on the soil microbiome in a laboratory incubation study. *Soil Biology and*
510 *Biochemistry*, 167, p.108605.

511 Behnamian, A., Millard, K., Banks, S.N., White, L., Richardson, M. and Pasher, J., 2017. A systematic
512 approach for variable selection with random forests: achieving stable variable importance values.
513 IEEE Geoscience and Remote Sensing Letters, 14(11), pp.1988-1992.

514 Bonan, G.B., 2008. Forests and climate change: forcings, feedbacks, and the climate benefits of
515 forests. *science*, 320(5882), pp.1444-1449.

516 Bond-Lamberty, B., Bailey, V.L., Chen, M., Gough, C.M. and Vargas, R., 2018. Globally rising soil
517 heterotrophic respiration over recent decades. *Nature*, 560(7716), pp.80-83.

518 Bray, J.R. and Curtis, J.T., 1957. An ordination of the upland forest communities of southern
519 Wisconsin. *Ecological monographs*, 27(4), pp.326-349.

520 Callahan, B.J., McMurdie, P.J., Rosen, M.J., Han, A.W., Johnson, A.J.A. and Dada, S.H., High-resolution
521 sample inference from Illumina amplicon data., 2016, 13. DOI: <https://doi.org/10.1038/nmeth.3869>, pp.581-583.

522 Caporaso, J.G., Lauber, C.L., Walters, W.A., Berg-Lyons, D., Lozupone, C.A., Turnbaugh, P.J., Fierer, N.
523 and Knight, R., 2011. Global patterns of 16S rRNA diversity at a depth of millions of sequences
524 per sample. *Proceedings of the national academy of sciences*, 108(supplement_1), pp.4516-4522.

525 Caporaso, J.G., Lauber, C.L., Walters, W.A., Berg-Lyons, D., Huntley, J., Fierer, N., Owens, S.M., Betley,
526 J., Fraser, L., Bauer, M. and Gormley, N., 2012. Ultra-high-throughput microbial community
527 analysis on the Illumina HiSeq and MiSeq platforms. *The ISME journal*, 6(8), pp.1621-1624.

528 Chatterjee, A., Vance, G.F., Pendall, E. and Stahl, P.D., 2008. Timber harvesting alters soil carbon
529 mineralization and microbial community structure in coniferous forests. *Soil Biology and*
530 *Biochemistry*, 40(7), pp.1901-1907.

531 Chi, J., Zhao, P., Klosterhalfen, A., Jocher, G., Kljun, N., Nilsson, M.B. and Peichl, M., 2021. Forest floor
532 fluxes drive differences in the carbon balance of contrasting boreal forest stands. *Agricultural and*
533 *Forest Meteorology*, 306, p.108454.



535 Fekete, I., Kotrczó, Z., Varga, C., Nagy, P.T., Várbíró, G., Bowden, R.D., Tóth, J.A. and Lajtha, K.,
536 2014. Alterations in forest detritus inputs influence soil carbon concentration and soil respiration
537 in a Central-European deciduous forest. *Soil Biology and Biochemistry*, 74, pp.106-114.

538 Gordon, A.M., Schlentner, R.E. and Cleve, K.V., 1987. Seasonal patterns of soil respiration and CO₂
539 evolution following harvesting in the white spruce forests of interior Alaska. *Canadian Journal of*
540 *Forest Research*, 17(4), pp.304-310.

541 Grace, J., 2004. Understanding and managing the global carbon cycle. *Journal of Ecology*, 92(2), pp.189-
542 202.

543 Halim, M.A., Bieser, J.M. and Thomas, S.C., 2024. Large, sustained soil CO₂ efflux but rapid recovery of
544 CH₄ oxidation in post-harvest and post-fire stands in a mixedwood boreal forest. *Science of The*
545 *Total Environment*, 930, p.172666.

546 Harel, A., Sylvain, J.D., Drolet, G., Thiffault, E., Thiffault, N. and Tremblay, S., 2023. Fine scale
547 assessment of seasonal, intra-seasonal and spatial dynamics of soil CO₂ effluxes over a balsam
548 fir-dominated perhumid boreal landscape. *Agricultural and Forest Meteorology*, 335, p.109469.

549 Jacinthe, P.A., 2015. Carbon dioxide and methane fluxes in variably-flooded riparian
550 forests. *Geoderma*, 241, pp.41-50.

551 Jorgenson, M.T., Douglas, T.A., Liljedahl, A.K., Roth, J.E., Cater, T.C., Davis, W.A., Frost, G.V., Miller,
552 P.F. and Racine, C.H., 2020. The roles of climate extremes, ecological succession, and hydrology
553 in repeated permafrost aggradation and degradation in fens on the Tanana Flats, Alaska. *Journal*
554 *of Geophysical Research: Biogeosciences*, 125(12), p.e2020JG005824.

555 Köljalg, U., Nilsson, R.H., Abarenkov, K., Tedersoo, L., Taylor, A.F., Bahram, M., Bates, S.T., Bruns,
556 T.D., Bengtsson-Palme, J., Callaghan, T.M. and Douglas, B., 2013. Towards a unified paradigm
557 for sequence-based identification of fungi.

558 Köster, E., Köster, K., Berninger, F., Aaltonen, H., Zhou, X. and Pumpanen, J., 2017. Carbon dioxide,
559 methane and nitrous oxide fluxes from a fire chronosequence in subarctic boreal forests of
560 Canada. *Science of the Total Environment*, 601, pp.895-905.

561 Köster, E., Köster, K., Berninger, F., Prokushkin, A., Aaltonen, H., Zhou, X. and Pumpanen, J., 2018.
562 Changes in fluxes of carbon dioxide and methane caused by fire in Siberian boreal forest with
563 continuous permafrost. *Journal of environmental management*, 228, pp.405-415.



564 Lei, Q., Yu, H. and Lin, Z., 2024. Understanding China's CO₂ emission drivers: Insights from random
565 forest analysis and remote sensing data. *Heliyon*, 10(7).

566 Lytle, D.E. and Cronan, C.S., 1998. Comparative soil CO₂ evolution, litter decay, and root dynamics in
567 clearcut and uncut spruce-fir forest. *Forest Ecology and Management*, 103(2-3), pp.121-128.

568 Martin, B.D., Witten, D. and Willis, A.D., 2021. Corncob: count regression for correlated observations
569 with the beta-binomial.

570 Marty, C., Piquette, J., Morin, H., Bussières, D., Thiffault, N., Houle, D., Bradley, R.L., Simpson, M.J.,
571 Ouimet, R. and Paré, M.C., 2019. Nine years of in situ soil warming and topography impact the
572 temperature sensitivity and basal respiration rate of the forest floor in a Canadian boreal
573 forest. *PLoS One*, 14(12), p.e0226909.

574 Mölder, F., Jablonski, K.P., Letcher, B., Hall, M.B., Tomkins-Tinch, C.H., Sochat, V., Forster, J., Lee, S.,
575 Twardziok, S.O., Kanitz, A., Wilm, A., Holtgrewe, M., Rahmann, S., Nahnsen, S., and Köster, J.
576 2021). Sustainable data analysis with Snakemake. *F1000Research* 10:33.
577 doi:10.12688/f1000research.29032.1

578 Montgomery, K., Williams, T.J., Brettle, M., Berengut, J.F., Ray, A.E., Zhang, E., Zaugg, J., Hugenholtz,
579 P. and Ferrari, B.C., 2021. Persistence and resistance: survival mechanisms of *Candidatus*
580 *Dormibacterota* from nutrient-poor Antarctic soils. *Environmental Microbiology*, 23(8), pp.4276-
581 4294.

582 Nilsson, R.H., Larsson, K.H., Taylor, A.F.S., Bengtsson-Palme, J., Jeppesen, T.S., Schigel, D., Kennedy,
583 P., Picard, K., Glöckner, F.O., Tedersoo, L. and Saar, I., 2019. The UNITE database for molecular
584 identification of fungi: handling dark taxa and parallel taxonomic classifications. *Nucleic acids
585 research*, 47(D1), pp.D259-D264.

586 Oksanen J, Simpson G, Blanchet F, Kindt R, Legendre P, Minchin P, O'Hara R, Solymos P, Stevens M,
587 Szoecs E, Wagner H, Barbour M, Bedward M, Bolker B, Borcard D, Carvalho G, Chirico M, De
588 Caceres M, Durand S, Evangelista H, FitzJohn R, Friendly M, Furneaux B, Hannigan G, Hill M,
589 Lahti L, McGlinn D, Ouellette M, Ribeiro Cunha E, Smith T, Stier A, Ter Braak C, Weedon J
590 (2024). *_vegan: Community Ecology Package_*. R package version 2.6-6.1, <<https://CRAN.R-project.org/package=vegan>>.

592 Pan, Y., Birdsey, R.A., Fang, J., Houghton, R., Kauppi, P.E., Kurz, W.A., Phillips, O.L., Shvidenko, A., Lewis,
593 S.L., Canadell, J.G. and Ciais, P., 2011. A large and persistent carbon sink in the world's
594 forests. *science*, 333(6045), pp.988-993.



595 Parada, A.E., Needham, D.M. and Fuhrman, J.A., 2016. Every base matters: assessing small subunit
596 rRNA primers for marine microbiomes with mock communities, time series and global field
597 samples. *Environmental microbiology*, 18(5), pp.1403-1414.

598 Parker, T.C., Clemmensen, K.E., Friggens, N.L., Hartley, I.P., Johnson, D., Lindahl, B.D., Olofsson, J.,
599 Siewert, M.B., Street, L.E., Subke, J.A. and Wookey, P.A., 2020. Rhizosphere allocation by
600 canopy-forming species dominates soil CO₂ efflux in a subarctic landscape. *New
601 Phytologist*, 227(6), pp.1818-1830.

602 Pribyl, D.W., 2010. A critical review of the conventional SOC to SOM conversion
603 factor. *Geoderma*, 156(3-4), pp.75-83.

604 Quast, C., Pruesse, E., Yilmaz, P., Gerken, J., Schweer, T., Yarza, P., Peplies, J. and Glöckner, F.O., 2012.
605 The SILVA ribosomal RNA gene database project: improved data processing and web-based
606 tools. *Nucleic acids research*, 41(D1), pp.D590-D596.

607 R-Core-Team, 2018. R: A Language and Environment for Statistical Computing, R Foundation for
608 Statistical Computing.

609 Rodtassana, C., Unawong, W., Yaemphum, S., Chanthorn, W., Chawchai, S., Nathalang, A., Brockelman,
610 W.Y. and Tor-ngern, P., 2021. Different responses of soil respiration to environmental factors
611 across forest stages in a Southeast Asian forest. *Ecology and Evolution*, 11(21), pp.15430-15443.

612 Schonlau, M. and Zou, R.Y., 2020. The random forest algorithm for statistical learning. *The Stata Journal*,
613 20(1), pp.3-29.

614 Smith, D.P. and Peay, K.G., 2014. Sequence depth, not PCR replication, improves ecological inference
615 from next generation DNA sequencing. *PloS one*, 9(2), p.e90234.

616 Soil Survey Staff. 2022. Keys to Soil Taxonomy, 13th edition. USDA Natural Resources Conservation
617 Service

618 Sprengel, C., 1827. Über Pflanzenhumus, Humussäure und humussaure Salze. *Archiv der
619 Pharmazie*, 21(3), pp.261-263.

620 Storer, D.A., 1984. A simple high sample volume ashing procedure for determination of soil organic
621 matter. *Communications in Soil Science and plant analysis*, 15(7), pp.759-772.



622 Turetsky, M.R., Abbott, B.W., Jones, M.C., Anthony, K.W., Olefeldt, D., Schuur, E.A., Grosse, G., Kuhry,
623 P., Hugelius, G., Koven, C. and Lawrence, D.M., 2020. Carbon release through abrupt permafrost
624 thaw. *Nature Geoscience*, 13(2), pp.138-143.

625 Vas, D.A., Corriveau, E.J., Gaimaro, L.W. and Barbato, R.A., 2023. Challenges and limitations of using
626 autonomous instrumentation for measuring in situ soil respiration in a subarctic boreal forest in
627 Alaska, USA. *ERDC/CRREL TR*, vols. 23–18.

628 Walters, W., Hyde, E.R., Berg-Lyons, D., Ackermann, G., Humphrey, G., Parada, A., Gilbert, J.A.,
629 Jansson, J.K., Caporaso, J.G., Fuhrman, J.A. and Apprill, A., 2016. Improved bacterial 16S rRNA
630 gene (V4 and V4-5) and fungal internal transcribed spacer marker gene primers for microbial
631 community surveys. *Msystems*, 1(1), pp.10-1128.

632 Watts, J.D., Natali, S.M., Minions, C., Risk, D., Arndt, K., Zona, D., Euskirchen, E.S., Rocha, A.V.,
633 Sonnentag, O., Helbig, M. and Kalhori, A., 2021. Soil respiration strongly offsets carbon uptake
634 in Alaska and Northwest Canada. *Environmental Research Letters*, 16(8), p.084051.

635 Webster, K.L., McLaughlin, J.W., Kim, Y., Packalen, M.S. and Li, C.S., 2013. Modelling carbon
636 dynamics and response to environmental change along a boreal fen nutrient gradient. *Ecological
637 Modelling*, 248, pp.148-164.

638 West, J.R., Whitman, T., 2022. Disturbance by soil mixing decreases microbial richness and supports
639 homogenizing community assembly processes. *FEMS Microbiology Ecology*, 98, 1–11.

640 Wickham, H. and Wickham, H., 2016. *Data analysis* (pp. 189-201). Springer International Publishing.

641 Willis, A., Bunge, J. and Whitman, T., 2017. Improved detection of changes in species richness in high diversity
642 microbial communities. *Journal of the Royal Statistical Society Series C: Applied Statistics*, 66(5),
643 pp.963-977.

644 Yilmaz, P., Parfrey, L.W., Yarza, P., Gerken, J., Pruesse, E., Quast, C., Schweer, T., Peplies, J., Ludwig, W. and
645 Glöckner, F.O., 2014. All-species Living Tree Project (LTP) taxonomic frameworks. *Nucleic Acids
646 Res*, 42, pp.D643-D648.